JOURNAL OF SYNCHROTRON RADIATION
ISSN 1600-5775

Study of the microstructure information of GaAs epilayers grown on silicon substrate using synchrotron radiation

Ravi Kumar,[a]* V. K. Dixit,[a] A. K. Sinha,[b] Tapas Ganguli,[b] C. Mukherjee,[c] S. M. Oak[a] and T. K. Sharma[a]*

[a]Semiconductor Physics and Devices Laboratory, Raja Ramanna Centre for Advanced Technology, Indore 452 013, India, [b]Indus Synchrotron Utilization Division, Raja Ramanna Centre for Advanced Technology, Indore 452 013, India, and [c]Mechanical and Optical Support Section, Raja Ramanna Centre for Advanced Technology, Indore 452 013, India. *Correspondence e-mail: ravi@rrcat.gov.in, tarun@rrcat.gov.in

Received 2 July 2015
Accepted 21 October 2015

Edited by G. E. Ice, Oak Ridge National Laboratory, USA

Keywords: HRXRD; Williamson–Hall analysis; GaAs epilayers; coherence length; tilt; twist.

Williamson–Hall (WH) analysis is a well established method for studying the microstructural properties of epilayers grown on foreign substrates. However, the method becomes inapplicable in specific cases where the structure factor considerations and the presence of anti-phase domains forbid the data acquisition for certain reflections in conventional high-resolution X-ray diffraction (HRXRD) measurements. Here, this limitation is overcome by exploiting the large intensity (25 μW mm^{-2}) and high photon energy (15.5 keV) of the X-ray beam obtained from a synchrotron radiation source. The lateral coherence length, vertical coherence length, tilt and micro-strain of GaAs epilayers grown on Si substrate have been successfully measured using the conventional WH analysis. The microstructure information obtained from the conventional WH analysis based on the data acquired at the synchrotron radiation source is in reasonable agreement with the results obtained from atomic force microscope and surface profiler measurements. Such information cannot be obtained on a laboratory-based HRXRD system where modification of the WH method by involving a set of parallel asymmetric crystallographic planes is found to be essential. However, the information obtained from the modified WH method is along a different crystallographic orientation.

1. Introduction

High-resolution X-ray diffraction (HRXRD) (Fewster, 1996, 2013; Ayers, 2007; Birkholz, 2006) is a well established non-destructive technique for studying the epitaxial layers grown on foreign substrates. HRXRD measurements are generally performed using laboratory X-ray sources based on copper/molybdenum X-ray tubes. Unfortunately, such X-ray tools offer a very limited range of intensity and wavelength. In this context, synchrotron radiation sources offer a great opportunity for the HRXRD measurements where a broad range of intensity and wavelength of X-ray radiation can be obtained. This indeed becomes extremely important for the cases where a few crucial reflections are either broadened due to structure factor considerations or are inherently weak for a particular crystallographic plane. In order to understand the microstructural properties of epitaxial layers though Williamson–Hall (WH) analysis, one needs to collect several diffraction patterns for a set of parallel symmetric crystallographic planes (Williamson & Hall, 1953; Neumann *et al.*, 1987; Moram & Vickers, 2009; Kumar *et al.*, 2011, 2014). WH analysis is an established method for studying the microstructure of epitaxial layers and has been successfully applied to various

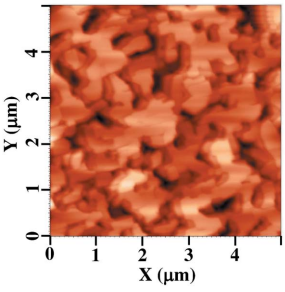

hetero-epitaxial systems like GaN/sapphire (Moram & Vickers, 2009; Vickers *et al.*, 2005; Lee *et al.*, 2005; Chierchia *et al.*, 2003), InN/sapphire (Zhu *et al.*, 2007; Ganguli *et al.*, 2008), ZnO/sapphire (Singh *et al.*, 2008), GaAs/Si (Neumann *et al.*, 1987; Kumar *et al.*, 2011, 2014), GaAs/Ge (Neumann *et al.*, 1987; Wong *et al.*, 2012) and GaP/Si (Dixit *et al.*, 2008). Under conventional WH analysis, micro-structural information related to grains is obtained where various parameters such as lateral coherence length (LCL), vertical coherence length (VCL), tilt (α), twist and micro-strain (ε) are experimentally measured. Recently, we extended the conventional WH method where a new set of parallel asymmetric crystallographic planes was taken to study the microstructure of GaAs epilayers grown on silicon substrates (Kumar *et al.*, 2011, 2014). The extended WH analysis was important since the conventional WH analysis failed to deliver the desired microstructure-related information of those epitaxial layers. This was due to the observance of a weak diffraction pattern for the (006) reflection that restricted the accuracy of the conventional WH analysis. The extended WH analysis provided the desired information related to the microstructure of GaAs epitaxial layers grown on Si. However, the acquisition of HRXRD data for asymmetric reflections is rather cumbersome. Precise multidirectional alignment of a sample is critical for the data acquisition of a diffraction pattern for asymmetric crystallographic planes. A goniometer with precise multidirectional movements is therefore essential for recording the data required for the extended WH analysis. Moreover, one probes the epilayer along a different crystallographic orientation under the modified WH method. Further, the intensity of the diffraction pattern might be really weak for some of the asymmetric reflections. On the other hand, large photon counts are usually recorded for symmetric reflections and even the data acquisition is relatively simpler. In view of this, it is desirable to find a set of reflections where diffraction patterns of reasonable intensity can be recorded. This is indeed possible at a synchrotron radiation source where the size of the limiting sphere can be varied by changing the wavelength of the X-rays. Moreover, the intensity of the incident X-ray beam at a synchrotron radiation source is very high (Sinha *et al.*, 2013) when compared with the laboratory-based sources. With this in mind, we present the WH analysis of GaAs epilayers grown on Si by performing HRXRD measurements on the Indus-2 synchrotron radiation source. It is found that the conventional WH analysis performed on a synchrotron radiation source is able to reveal the desired information related to the microstructure of GaAs epilayers grown on Si which is in reasonable agreement with the results obtained from atomic force microscope (AFM) measurements.

Epitaxial growth of group III/V material, *e.g.* GaAs on Si, imposes a formidable challenge due to the high lattice constant mismatch, large thermal expansion coefficients difference and anti-phase domains issue (Neumann *et al.*, 1987; Kumar *et al.*, 2011; Georgakilas *et al.*, 1992; Sheldon *et al.*, 1988). The lattice constant mismatch and difference in the thermal expansion coefficients between GaAs and Si is 4.1% and 3.43×10^{-6} K^{-1}, respectively (Sheldon *et al.*, 1988). Thus, this material combination is prone to a high density of dislocations leading to the mosaicity of epilayers. Here, WH analysis provides useful information related to the microstructure. The combination of well developed Si technology with group III/V semiconductors like GaAs, GaP and InP opens up the possibility for a wide range of optoelectronic devices; for example, integrated light emitting diodes, laser diodes, detectors and solar cells on Si substrates (Neumann *et al.*, 1987; Dixit *et al.*, 2008).

2. Experimental details

GaAs epilayers were grown by the two-step growth method in a horizontal metal organic vapour phase epitaxy reactor (AIX-200) system. Trimethyl gallium and arsine gas were used as precursors. Prior to growth, Si substrates were cleaned using a modified Radio Corporation of America (RCA) cleaning method (Dixit *et al.*, 2008). Afterwards the substrate was preheated to 870°C for 30 min in a hydrogen (H_2) flow of $\sim$8 slpm (slpm = standard litres per minute). This is desired for promoting Si surface rearrangement and also for the removal of native oxide from Si substrate. This procedure for the removal of native oxide from Si wafers is found to be very successful where it is reported that the native oxide on Si wafer would not reappear even after 1–2 h (Meyer, 2001). After pre-heating the Si wafer at 870°C in the presence of H_2 for 30 min, the temperature was reduced to 450°C in the presence of a high flow of arsine. At this temperature, a GaAs nucleating layer of thickness $\sim$60 nm with a V/III ratio $\simeq$ 340 was grown. This was followed by the growth of a GaAs layer of thickness $\sim$250 nm at 670°C with V/III ratio $\simeq$ 100.

The laboratory-source-based HRXRD measurements were performed using the PANalytical X'prt PRO MRD system. The system with Cu target and hybrid monochromator (Göbel's mirror with a four-bounce crystal monochromator) gives a Cu $K\alpha_1$ beam with beam divergence of $\sim$20 arcsec. A three-bounce collimator (also referred to as a triple-axis attachment) is placed in front of the detector to ensure an acceptance angle of 12 arcsec. The synchrotron-based HRXRD measurements were performed using the angle-dispersive X-ray diffraction beamline (BL-12) (Sinha *et al.*, 2013) at the Indus-2 synchrotron radiation source of RRCAT, Indore. The beamline consists of a Si (311) based double-crystal monochromator with bendable focusing optics. HRXRD measurements at Indus-2 are performed at 15.5 keV using a scintillator detector having 75 arcsec opening in the diffraction plane. Note that the full width at half-maxima (FWHM) of HRXRD patterns is typically one order larger than the instrumental broadening. Hence, it is neglected in the data analysis (Ayers, 1994). Two independent sets of X-ray diffraction patterns are recorded using the respective laboratory and synchrotron sources. ω and ω-2θ scans for the (00L) reflections (L = 2, 4, 6 *etc.*) of GaAs were performed using the synchrotron radiation and laboratory sources, respectively. Here, ω is defined as the angle between the incident X-ray beam and the sample surface while 2θ is the angle between the

incident and diffracted X-ray beams. The ω and ω-2θ directions explore the Ewald sphere in different directions as shown in Fig. 1, where a ω (ω-2θ) scan provides the lateral (vertical) information of the epilayer. AFM measurements are performed using a multimode scanning probe microscope (NT-MDT, SOLVER-PRO). Silicon cantilever tips of radius of curvature 10 nm, resonant frequency 190 kHz and spring constant 5.5 N m^{-1} are used in non-contact mode. The thickness of the epilayers is determined by a surface profiler model Alpha-step IQ (KLA Tencor). A step was made by selectively etching the GaAs layer on the silicon substrate (Georgakilas *et al.*, 1992).

3. Data analysis procedure

In conventional WH analysis, diffracting planes parallel to the growth plane, *i.e.* symmetric planes, are used. The recorded data are converted into reciprocal lattice units (rlu), *i.e.* q_x and q_z, using the following formulae (Birkholz, 2006; Als-Nielsen & McMorrow, 2011),

$$q_x = \lambda^{-1}[\cos\omega - \cos(2\theta - \omega)], \quad (1a)$$

$$q_z = \lambda^{-1}[\sin\omega + \sin(2\theta - \omega)], \quad (1b)$$

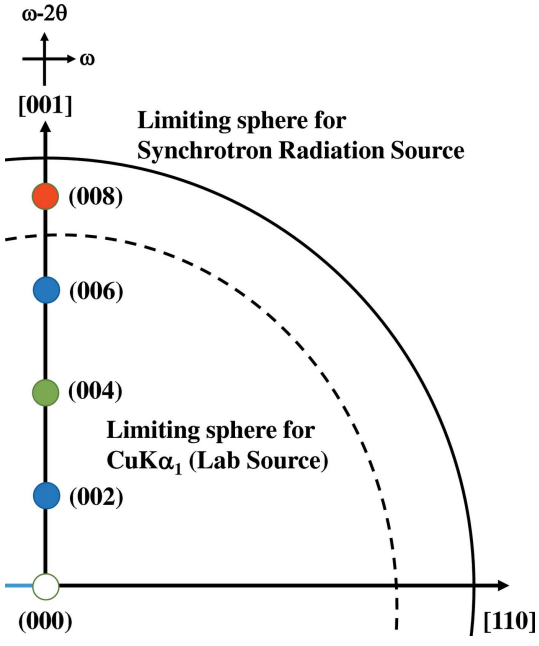

Figure 1
Schematic of the portion of the limiting sphere to illustrate the allowed symmetric reflections for GaAs grown on (001) Si substrates. Here, the [110] direction lies in the growth plane. The limiting sphere governed by the wavelength of the laboratory X-ray source (Cu $K\alpha_1$) is shown by a dashed line (red) whereas the limiting sphere governed by the wavelength of synchrotron radiation is shown by a solid line (green). Note that the (008) reflection (red filled circle) is accessible only when HRXRD measurements are performed at the synchrotron radiation source. At 15.5 keV energy a few more reflections are accessible. However, the reflections only up to (008) are shown here for simplicity. ω is defined as the angle which the incident X-ray beam makes with the sample surface while 2θ is the angle between the incident and diffracted X-ray beams.

where λ is the X-ray wavelength, and ω and 2θ are the angle of incidence and the angle of diffraction, respectively. Thereafter, the pseudo-Voigt fit (Moram & Vickers, 2009; Kumar *et al.*, 2011) of the converted data is carried out where the fraction of Lorentzian component (f) and FWHM, *i.e.* Δq_x and Δq_z, are obtained for ω and ω-2θ scans, respectively. The Lorentzian component (f) is related to a constant n by the following relation,

$$n = 1 + (1 - f)^2. \quad (2)$$

Then a linear fit of the respective values of the FWHM for ω and ω-2θ scans is made using the following formulae,

$$(\Delta q_x)^n = (\Delta q_{\rm LCL})^n + (\alpha q)^n, \quad (3a)$$

$$(\Delta q_z)^n = (\Delta q_{\rm VCL})^n + (\varepsilon q)^n. \quad (3b)$$

From this exercise, the values of LCL and tilt can be obtained from a set of ω scans while the value of VCL and micro-strain are obtained from ω-2θ scans. It is obvious that at least three symmetric reflections are required for a good accuracy of WH analysis. As mentioned in our earlier article, the accuracy of conventional WH analysis is limited by the strength of the (006) symmetric reflection for the GaAs epilayers grown on Si (Kumar *et al.*, 2014).

The crystallographic planes that can be accessed in HRXRD measurements are determined by the wavelength (λ) of the X-ray radiation source. This is described by drawing a limiting sphere of '2/λ' radius as shown in Fig. 1. The limiting sphere for the laboratory XRD systems based on Cu $K\alpha_1$ (λ = 1.54056 Å) is shown in Fig. 1 where one can access only the (002), (004) and (006) set of symmetric planes. Note that there are many asymmetric reflections that are also accessible by the same X-ray source. However, we are interested only in the symmetric reflections for the conventional WH analysis. The radius (2/λ) of the limiting sphere can be enlarged by increasing the energy of the incident X-ray beam at the synchrotron radiation source as shown in Fig. 1. It is obvious that now even the (008) symmetric reflection can be accessed that can be used to improve the accuracy of conventional WH analysis. Furthermore, the enormous intensity of the X-ray beam at a synchrotron radiation source considerably helps to improve the signal-to-noise (S/N) ratio.

4. Results and discussion

Fig. 2 shows ω and ω-2θ scans recorded for various symmetric reflections using the laboratory- and synchrotron-based X-ray sources. Note that the FWHM of the respective diffraction patterns that are recorded at two separate HRXRD systems are almost similar. This is obvious since the plots are made while keeping the x-axis in reciprocal lattice units instead of ω or ω-2θ. Furthermore, the diffraction pattern for the (006) reflection recorded by the laboratory source is very weak and cannot be used in WH analysis. On the other hand, the same pattern recorded by the synchrotron radiation source has a very good S/N ratio that makes it reasonable for WH analysis. As mentioned earlier, the wavelength of a synchrotron

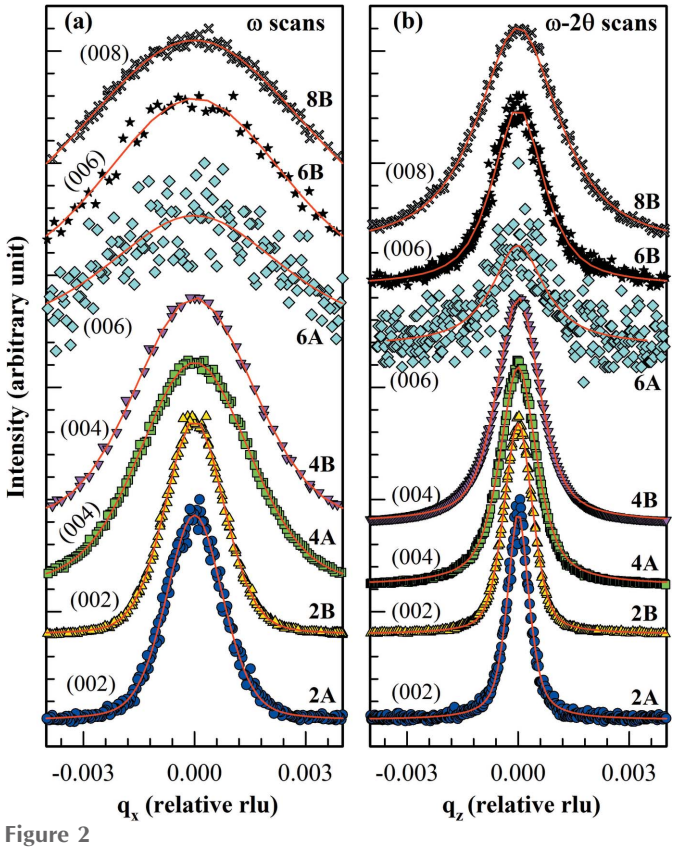

Figure 2
HRXRD pattern of GaAs epilayer grown on Si substrate: (*a*) ω scans, (*b*) ω-2θ scans, where the curves labelled as 2A (2B), 4A (4B) and 6A (6B) are the diffraction patterns for the (002), (004), (006) reflections acquired using the laboratory (synchrotron) based X-ray source. Note that the (008) scans are acquired only at the synchrotron radiation source. The overlaying solid lines show the pseudo-Voigt fitting of the experimental data.

radiation source is tunable which in fact enabled us also to record the diffraction pattern for the (008) reflection. Such a diffraction pattern cannot be recorded by using a laboratory source equipped with Cu X-ray tube. This reflection can also be probed by a molybdenum-based X-ray source. However, a Cu $K\alpha_1$ X-ray source is generally preferred for investigating the conventional III/V semiconductors because Cu $K\alpha_1$ interacts with matter more strongly than Mo $K\alpha_1$, leading to brighter diffraction spots. It can be easily appreciated that the availability of HRXRD data for four symmetric reflections is extremely important for the accuracy of microstructure information obtained from conventional WH analysis.

Next, the data shown in Fig. 2 are analyzed by following the procedure described in §3. It is observed that a low (high) value of '*f*' is recorded for the ω (ω-2θ) scans. A low (high) value of '*f*' along the ω (ω-2θ) direction indicates that the Lorentzian component of the broadening is low (high) along the lateral (vertical) directions. Note that the Lorentzian component of the broadening is governed by the theoretical broadening of the crystal while the Gaussian component of the broadening is decided by the crystal imperfections and inhomogeneities. Hence, a large value of '*f*' extracted from (ω-2θ) scans indicates a large grain size along the vertical direction while a low value of '*f*' extracted from the ω scans shows a small grain size in the lateral direction. This indicates the presence of a large number of defects and dislocations in the lateral direction. In the case of the GaAs/Si (001) material system, the majority of dislocations are of 60° mixed dislocations (Ayers, 2007; Kumar *et al.*, 2014; Qiu *et al.*, 2007). Burgers vectors of 60° mixed dislocations have three major components, namely misfit, screw and tilt (Ayers, 2007; Kumar *et al.*, 2014; Qiu *et al.*, 2007). While the tilt components of the dislocations lie primarily along the [001] direction, the misfit and screw dislocation components lie along the ⟨110⟩ directions. Because of this, one expects to observe a large number of dislocations in the growth plane which is the primary reason for the large broadening of the ω scans and also the low value of '*f*'.

Fig. 3 shows the WH plots for ω and ω-2θ scans recorded using the synchrotron radiation source. The FWHM values estimated from the line-shape analysis of the data shown in Fig. 2 are plotted in Fig. 3 where Δq_x (Δq_z) represents the FWHM of the ω (ω-2θ) scans for the corresponding symmetric reflections. The intercept on the *y*-axis is related to the value of LCL (VCL) which is obtained from the plot of Δq_x^n (Δq_z^n) *versus* q^n. Similarly, the slopes of the two curves provide the values of tilt and micro-strain, respectively. These values are summarized in Table 1. Fig. 4(*a*) shows the AFM image of the same sample. The formation of grains of different sizes and the grain boundaries are clearly observed in the AFM image. The observed mosaic nature of the sample is expected because of the large lattice constant and thermal constant mismatches between the layer and substrate. Fig. 4(*b*) shows the variation of the size of grains *versus* frequency (number of grains of the same size) of the sample which is obtained for the image analysis of AFM data. A large majority of grains are of size smaller than 0.6 µm whereas only a few grains of size larger than 1 µm are seen. The value of LCL estimated from WH

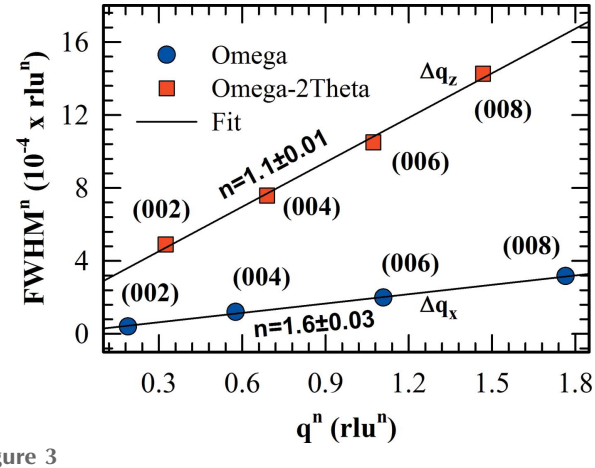

Figure 3
Williamson–Hall plots prepared using ω and ω-2θ scans for (002), (004), (006) and (008) symmetric reflections recorded using the Indus-2 synchrotron radiation source. The size of the error bars is smaller than the size of symbols. The value of *n* is 1 for the Lorentzian component and 2 for the Gaussian component; $1 < n < 2$ whenever the line shape is defined by a pseudo-Voigt profile.

Table 1
Summary of the microstructure of GaAs epilayers grown on Si substrate.

The values of lateral coherence length (LCL), vertical coherence length (VCL), tilt and micro-strain are obtained by performing the Williamson–Hall analysis of HRXRD data acquired at the Indus-2 synchrotron radiation source. The values of grain size and layer thickness measured by atomic force microscopy and surface profiler techniques are also included for comparison purposes.

Epilayer thickness (μm)	Grain size (μm)	LCL WH (μm)	VCL WH (μm)	Tilt WH (°)	Micro-strain WH (%)
0.31	0.40 ± 0.05	0.11 ± 0.005	0.24 ± 0.08	0.27 ± 0.01	0.15 ± 0.1

analysis is lower than the grain size obtained from AFM measurements, which can be easily understood since the value of LCL is related to the grain size where atoms coherently scatter X-rays. Moreover, AFM provides microscopic information related to the topography of the sample whereas HRXRD delivers crucial information related to the crystalline quality. Similar trends are also reported by other researchers (Dixit *et al.*, 2008; Pal *et al.*, 2015; Yadav *et al.*, 2008). Furthermore, the thickness of the GaAs layer measured from the surface profiler is about 0.31 μm. The value of VCL measured from WH analysis is lower than the layer thickness which is also expected because of the formation of defects and dislocations at the GaAs–Si heterointerface. Note that the value of VCL is correlated with the part of the layer thickness where atoms coherently scatter the X-ray radiation. A small VCL clearly indicates a poor quality of heterointerface, which is expected due to the large lattice mismatch between the layer and substrate. Note that the intensity of the synchrotron radiation source in our experiments was about 25 μW mm^{-2}. GaAs is a radiation-hard material (Owens & Peacock, 2004) which makes it a potential candidate for the development of detectors for high-flux X-ray imaging applications (Lozinskaya *et al.*, 2014; Veale *et al.*, 2014). No structural change in the sample was observed after exposure to the synchrotron radiation. AFM images were also recorded before and after the exposure where no change in the sample topography was observed.

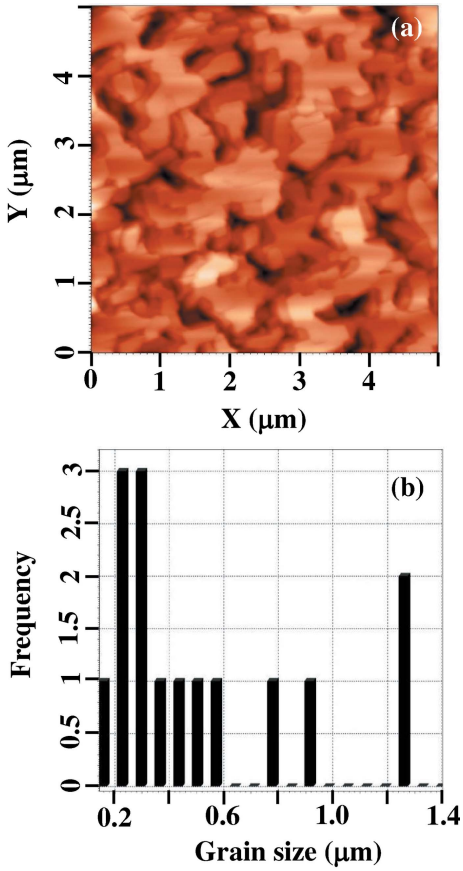

Figure 4
(*a*) AFM image (5 μm × 5 μm) of the GaAs epilayer grown on Si substrate, and (*b*) frequency distribution of the grain size obtained from the image analysis of AFM data.

5. Conclusion

Conventional WH analysis based on the HRXRD data acquired on a synchrotron radiation source is used to find the microstructure of GaAs epilayers grown on Si substrates where the values of LCL, VCL, tilt and the micro-strain are successfully measured. This information could not be obtained by performing similar experiments on a laboratory-based X-ray diffraction system. The high intensity and high energy of the incident X-ray beam, delivered by the Indus-2 synchrotron radiation source, are the two critical parameters for these measurements. The values of LCL (VCL) are lower than the average grain size (layer thickness) obtained from AFM (surface profiler) measurements. This indicates the moderate crystalline quality of the epitaxial film, which is expected due to the lattice constant/thermal expansion coefficient differences between the layer and substrate. Although we have investigated GaAs epilayers grown on silicon substrates as an example, the proposed method is in general applicable for other semiconductor epilayers grown on foreign substrates.

Acknowledgements

The authors thank Dr M. P. Joshi and Dr Rajmohan for the thickness measurements, Mr U. K. Ghosh and Mr A. Khakha for their help during the growth of the samples, and Dr A. Sagdeo, Mr A. Upadhyay and Mr M. N. Singh for their help in the HRXRD measurements on beamline BL-12. The authors also acknowledge Dr P. D. Gupta, Director of RRCAT, for the constant support during the course of this work.

References

Als-Nielsen, J. & McMorrow, D. (2011). *Elements of Modern X-ray Physics*, 2nd ed. Wiley-VCH Verlag GmbH.
Ayers, J. E. (1994). *J. Cryst. Growth*, **135**, 71–77.
Ayers, J. E. (2007). *Heteroepitaxy of Semiconductors*, pp. 7–74. New York: CRC Press.
Birkholz, M. (2006). *Thin Film Analysis by X-ray Scattering*. Wiley-VCH Verlag GmbH.
Chierchia, R., Böttcher, T., Heinke, H., Einfeldt, S., Figge, S. & Hommel, D. (2003). *J. Appl. Phys.* **93**, 8918–8925.

Dixit, V. K., Ganguli, T., Sharma, T. K., Singh, S. D., Kumar, R., Porwal, S., Tiwari, P., Ingale, A. & Oak, S. M. (2008). *J. Cryst. Growth*, **310**, 3428–3435.
Fewster, P. F. (1996). *Rep. Prog. Phys.* **59**, 1339–1407.
Fewster, P. F. (2013). *X-ray Scattering from Semiconductors and Other Materials.* Singapore: World Scientific.
Ganguli, T., Kadir, A., Gokhale, M., Kumar, R., Shah, A. P., Arora, B. M. & Bhattacharya, A. (2008). *J. Cryst. Growth*, **310**, 4942–4946.
Georgakilas, A., Panayotatos, P., Stoemenos, J., Mourrain, J.-L. & Christou, A. (1992). *J. Appl. Phys.* **71**, 2679.
Kumar, R., Ganguli, T., Chouhan, V., Dixit, V. K., Mondal, P., Srivastava, A. K., Mukherjee, C. & Sharma, T. K. (2014). *J. Nano-Electron. Phys.* **6**, 02010.
Kumar, R., Ganguli, T., Chouhan, V. & Dixit, V. K. (2011). *J. Nano-Electron. Phys.* **3**, 17.
Lee, S. R., West, A. M., Allerman, A. A., Waldrip, K. E., Follstaedt, D. M., Provencio, P. P., Koleske, D. D. & Abernathy, C. R. (2005). *Appl. Phys. Lett.* **86**, 241904.
Lozinskaya, A. D., Novikov, V. A., Tolbanov, O. P., Tyazhev, A. & Zarubin, A. N. (2014). *J. Instrum.* **9**, C12047.
Meyer, D. J. (2001). *Silicon Epitaxy*, ch. 10, *Semiconductors and Semimetals*, Vol. 72. New York: Academic Press.
Moram, M. A. & Vickers, M. E. (2009). *Rep. Prog. Phys.* **72**, 036502.
Neumann, D. A., Zabel, H., Fischer, R. & Morkoç, H. (1987). *J. Appl. Phys.* **61**, 1023.
Owens, A. & Peacock, A. (2004). *Nucl. Instrum. Methods Phys. Res. A*, **531**, 18–37.
Pal, S., Singh, S. D., Dixit, V. K., Sharma, T. K., Kumar, R., Sinha, A. K., Sathe, V., Phase, D. M., Mukherjee, C. & Ingale, A. (2015). *J. Alloys Compd.* **646**, 393–398.
Qiu, Y., Li, M., Liu, G., Zhang, B., Wang, Y. & Zhao, L. (2007). *J. Cryst. Growth*, **308**, 325–329.
Sheldon, P., Jones, K. M., Al-Jassim, M. M. & Yacobi, B. G. (1988). *J. Appl. Phys.* **63**, 5609.
Singh, S., Kumar, R., Ganguli, T., Srinivasa, R. S. & Major, S. S. (2008). *J. Cryst. Growth*, **310**, 4640–4646.
Sinha, A. K., Sagdeo, A., Gupta, P., Upadhyay, A., Kumar, A., Singh, M. N., Gupta, R. K., Kane, S. R., Verma, A. & Deb, S. K. (2013). *J. Phys. Conf. Ser.* **425**, 072017.
Veale, M. C., Bell, S. J., Duarte, D. D., French, M. J., Schneider, A., Seller, P., Wilson, M. D., Lozinskaya, A. D., Novikov, V. A., Tolbanov, O. P., Tyazhev, A. & Zarubin, A. N. (2014). *Nucl. Instrum. Methods Phys. Res. A*, **752**, 6–14.
Vickers, M. E., Kappers, M. J., Datta, R., McAleese, C., Smeeton, T. M., Rayment, F. D. G. & Humphreys, C. J. (2005). *J. Phys. D*, **38**, A99.
Williamson, G. K. & Hall, W. H. (1953). *Acta Metall.* **1**, 22–31.
Wong, C. S., Bennett, N. S., Galiana, B., Tejedor, P., Benedicto, M., Molina-Aldareguia, J. M. & McNally, P. J. (2012). *Semicond. Sci. Technol.* **27**, 115012.
Yadav, B. S., Singh, S., Ganguli, T., Kumar, R., Major, S. S. & Srinivasa, R. S. (2008). *Thin Solid Films*, **517**, 488–493.
Zhu, X. L., Guo, L. W., Yu, N. S., Yan, J. F., Peng, M. Z., Zhang, J., Jia, H. Q., Chen, H. & Zhou, J. M. (2007). *J. Cryst. Growth*, **306**, 292–296.